The 'H2' optical transition in diamond: the effects of uniaxial stress perturbations, temperature and isotopic substitution

1992 J. Phys.: Condens. Matter 4 3439

(http://iopscience.iop.org/0953-8984/4/13/008)

J. Phys.: Condens. Matter 4 (1992) 3439–3452. Printed in the UK

The 'H2' optical transition in diamond: the effects of uniaxial stress perturbations, temperature and isotopic substitution

S C Lawson†, Gordon Davies, A T Collins and Alison Mainwood
Physics Department, King's College London, The Strand, London WC2R 2LS, UK

Received 6 December 1991

Abstract. Uniaxial stress perturbations establish the 1.257 eV 'H2' zero-phonon line as an electric-dipole allowed transition at the centre of a C_{2v} point group. Taken in conjunction with a simple one-electron model, the magnitudes of the perturbations support recent suggestions that the H2 centre is a negative charge state of the well-known nitrogen–vacancy–nitrogen 'H3' centre. The H2 zero-phonon line is 0.9 meV higher in energy in ^{13}C diamond than in ^{12}C diamond. The shift is consistent, within large uncertainties, with the shift expected from the temperature dependence of the line. A local vibrational mode involving predominantly *carbon* atoms is identified.

1. Introduction

The 'H2' vibronic band, with its zero-phonon line at 1.257 eV, was reported by Clark *et al* (1956) in the first systematic study of radiation damage in diamond. The band was observed as a very weak absorption feature in some natural diamonds which had been irradiated and annealed at 900 °C for 10 h; it was so weak that the zero-phonon line was not observed. Only relatively recently has it been shown that strong H2 absorption can be obtained; the procedure (Satoh 1988) uses synthetic diamonds which contain isolated substitutional nitrogen atoms. The diamonds are irradiated with a large dose of 4 MeV electrons, and then annealed, under pressure to prevent graphitization, at very high temperatures (typically 1750 °C at 5 GPa for 17 h). Transient capture of the vacancies by the single nitrogen atoms considerably enhances the diffusion of nitrogen through the diamond (Collins 1980). Some of the nitrogen atoms undergo self-trapping to form pairs of nearest neighbour substitutional nitrogen atoms, N–N. The N–N centre is known to be able to capture a vacancy and restructure into an N–V–N complex, producing the well-known 'H3' centre (Davies 1977). In addition, this procedure creates a strong H2 band (figure 1(a)).

Mita *et al* (1990) have shown that optical bleaching allows the equilibrium between the H2 and H3 bands to be temporarily changed. They suggest that the H2 band is produced by the negative charge state of the N–V–N complex, and the H3 band by the neutral charge state. In the treated synthetic diamonds, the negative charge state is obtained by charge compensation of the N–V–N centres from the remaining single nitrogen atoms, which are known to act as donors with an ionization energy of 1.7 eV

† Present address : National Institute for Research in Inorganic Materials, 1-1 Namiki, Tsukuba, Ibaraki 305, Japan.

0953-8984/92/133439+14$04.50

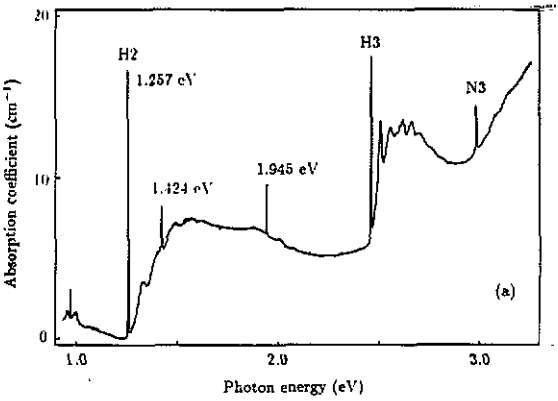

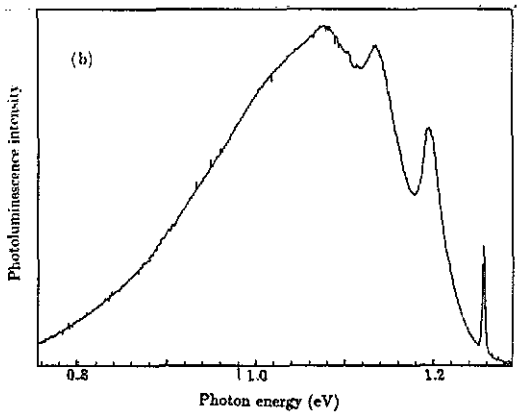

Figure 1. (a) Absorption recorded at 77 K of the near-infrared and visible spectral regions of a synthetic diamond after treatment to generate H2 centres. The treatment also produces H3 and N3 centres plus absorption at 1.945 eV produced by N–V centres. The 1.424 eV line is associated with a local vibrational mode of the H2 centre. (b) H2 photoluminescence spectrum, recorded at 77 K after correction for the wavelength-dependent response of the spectrometer system. The zero-phonon line observed in luminescence is reduced from its true intensity by strong absorption in the resonant zero-phonon absorption line.

(Farrer 1969). In most natural diamonds, the nitrogen atoms are preponderantly aggregated into N–N centres which have a larger ionization energy than the single N atoms. In these diamonds, N–V–N centres created by irradiation and annealing are in the neutral charge state and produce the H3 band.

In this paper we show, by uniaxial stress perturbations, that the point group of the H2 optical centre is C_{2v}, the same as for the H3 centre (Davies *et al* 1976). We report the temperature dependence of the band and use it to analyse the effect of changing the isotope of carbon in the lattice. For the first time in diamond we identify a local mode of vibration at a vacancy-related centre. An extension of the Lowther (1984) atomic-orbital model of vacancy centres in diamond supports the link between the H2 and H3 centres.

2. Experimental techniques

Most of the work has been carried out using diamonds synthesized by Sumitomo Electric Industries. The samples initially contained 2.6×10^{19} cm^{-3} isolated nitrogen atoms. They were irradiated with 10^{19} 4 MeV electrons cm^{-2}, and annealed at 1700 °C for 50 h under a stabilizing pressure of 5 GPa. To investigate the effects of changing the isotope of the host lattice, a diamond was synthesized from 99% ^{13}C by the Japanese National Institute for Research in Inorganic Materials. This diamond had an initial nitrogen concentration of 1.5×10^{19} cm^{-3}. It was irradiated with 5×10^{18} cm^{-2} 2 MeV electrons and heated under pressure as above.

Spectroscopic measurements have been made with a Spex $\frac{3}{4}$m dispersive spectrometer, fitted with a Northcoast germanium detector for the near-infrared spectral region or an RCA 31034A photomultiplier for the visible region. Photoluminescence was generated using the 1.916 eV line of a krypton laser. Uniaxial stresses were applied with the samples near liquid nitrogen temperature. Temperature data on the bandshapes were obtained between 10 and 80 K using an Oxford Instruments helium flow cryostat and from 77 to 400 K using the boil-off gas from a liquid nitrogen reservoir. For measurements at 2 K the samples were immersed in liquid helium pumped below its λ point.

3. General appearance of the band

With the exception of a preliminary report of this work (Lawson *et al* 1990) there are no detailed published spectra of the H2 band. Figure 1(a) shows the near infrared and visible absorption spectrum of a synthetic diamond after treatment to generate H2 centres. This treatment also produces H3 centres and 'N3' centres (a complex involving three nitrogen atoms (Shcherbakova and Sobolev 1972)); the H3 and N3 absorption features are labelled on figure 1(a). A detailed H2 photoluminescence spectrum is shown in figure 1(b). The zero-phonon line is at 1.257 eV. In absorption the one-phonon sideband peaks at 66 ± 3 meV from the zero-phonon line, while in photoluminescence it is only 62 ± 2 meV below the zero-phonon line. It is usual in the vacancy-related centres of diamond for the vibrational quanta observed in the absorption band to be higher than those in the luminescence band. For example, in the 1.945 eV N–V band the one-phonon sidebands peak at 68.5 meV in absorption and at 64 meV in luminescence (Davies and Hamer 1976). For the H3 band, the corresponding figures are 44.1 ± 0.5 meV and 41.4 ± 0.5 meV (Davies *et al* 1976).

In absorption the H2 zero-phonon line is always accompanied by a sharp spectral feature at 1.424 eV, 167.1 ± 0.05 meV higher in energy than the zero-phonon line (figure 1(a)). We will show that this feature is a phonon sideband of the H2 centre involving a local vibrational mode even though no corresponding feature is observed in photoluminescence.

No cathodoluminescence was observed from the H2 band in the sample used for figure 1(a), under conditions which generated easily observable cathodoluminescence from the H3 band in the same specimen.

4. Uniaxial stress perturbations

Uniaxial compressions have been applied along, in turn, the ⟨001⟩, ⟨111⟩ and ⟨110⟩ axes of diamonds held at about 80 K. The response of the zero-phonon absorption

line is shown in figure 2 for light whose electric vector is polarized parallel ('π') and perpendicular ('σ') to the stress axis. All the stress-split components have energies which change linearly in the applied stress (figure 3(a)) and their intensities are constant for all stresses. The 1.424 eV line splits into the same number of components as the zero-phonon line, with the same polarizations and essentially the same changes in energy (figure 3(b)). The two sets of data may therefore be analysed simultaneously.

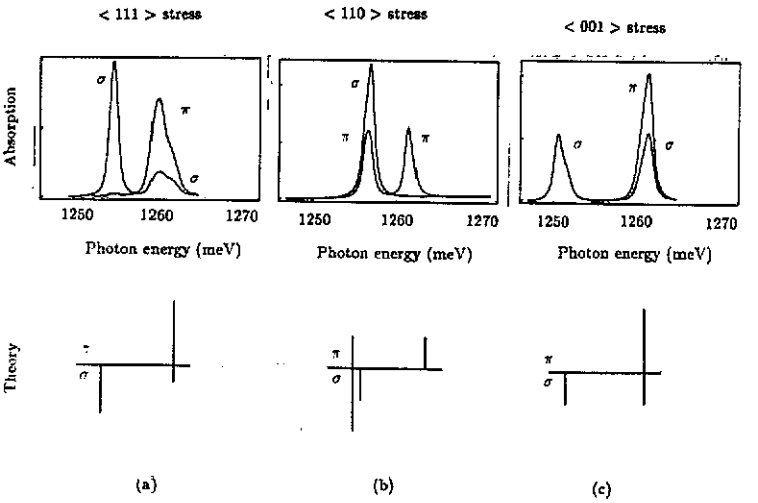

Figure 2. Absorption spectra recorded at about 80 K for the H2 zero-phonon line under uniaxial compressions of (a) 0.61 GPa parallel to ⟨111⟩, (b) 0.42 GPa parallel to [110] and (c) 0.66 GPa parallel to ⟨001⟩. The spectra have been recorded with light linearly polarized with its electric vector parallel ('π') and perpendicular ('σ') to the applied stress. For [110] stress the σ polarization has electric vector parallel to [$\bar{1}$10]. (The [001] polarization shows two equal intensity lines). At the bottom the spike spectra show the theoretical intensities (by the lengths of the spikes) of the π and σ polarizations for each stress axis.

The experimental data are consistent with ⟨110⟩ allowed-electric-dipole transitions at a rhombic I centre (Kaplyanskii 1964). Theoretical intensities (shown by the spike spectra in figure 2) for this type of transition compare closely with the measured polarized spectra. In the diamond structure a rhombic I centre has the C_{2v} point group with the C_2 axis along a ⟨001⟩ axis. A ⟨110⟩ electric dipole transition can occur between a state whose irreducible representation is A_1 or A_2 and a B_1 or B_2 state. Uniaxial stresses are unable to distinguish between these transitions or show which is the ground state.

For a quantitative discussion of the energy perturbations we define a right-handed orthogonal set of local coordinates X, Y, Z for each of the six inequivalent orientations of the C_{2v} centres such that Z is parallel to the C_2 axis, and X and Y are perpendicular to the two reflection planes of the centre. For example, for the orientation whose C_2 axis is aligned along [001] we define $Z \parallel [001]$, $X \parallel [110]$, and $Y \parallel [\bar{1}10]$. The strains used in the experiments are small (less than 10^{-3}) and so the perturbation to the Hamiltonian is limited to terms which are linear in the strain (or the applied stress). The linear stress dependence of the energies and the constant intensities of the stress-split components show that there are no stress-induced interactions of either the ground or the excited states with other nearby electronic

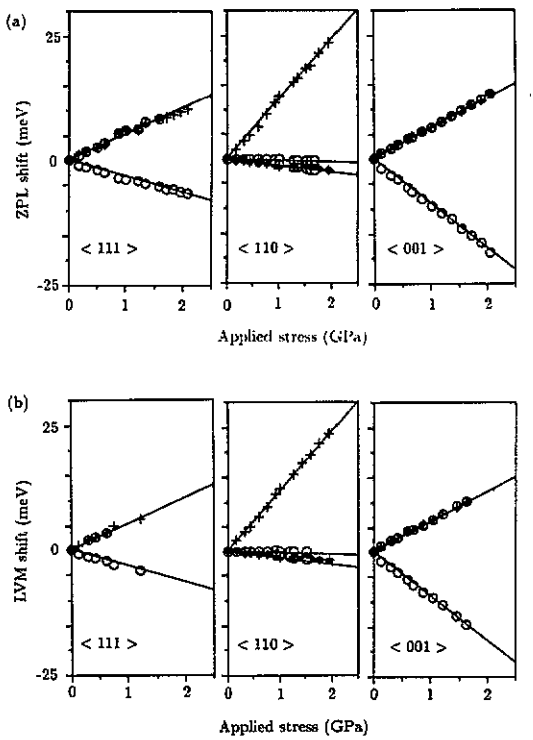

Figure 3. Points show the measured energies of the stress-split components of (a) the zero-phonon line and (b) the 1.424 eV line for ⟨111⟩, ⟨110⟩ and ⟨001⟩ compressions. Data measured with electric vector parallel to the stress axis are shown by + and perpendicular by o. The lines are the fit of the theory of section 4 with the parameters of table 1.

states. Since all the irreducible representations of the C_{2v} point group are singly dimensioned, first-order perturbations only arise from the stresses which transform as A_1 (i.e. those with stress tensor components s_{XX},s_{YY} or s_{ZZ} in the local axes X, Y and Z). In the commonly used notation of Kaplyanskii, the change $\Delta h\nu$ in energy of the optical transition is determined by three parameters A_1, A_2 and A_3. In terms of stress tensor components s_{xx}, s_{yy} or s_{zz} defined with respect to the crystal's axes x, y and z, for the centre oriented as defined above

$$\Delta h\nu = A_1 s_{zz} + A_2(s_{xx} + s_{yy}) + 2A_3 s_{xy}. \tag{1}$$

A least-squares fit to the seven measured energy perturbations of the zero-phonon line using the three adjustable parameters is shown by the lines in figure 3(a). The parameters are listed in table 1. The same parameters fit the energies of the 1.424 eV line (figure 3(b)).

The similar stress-dependence of the 1.424 eV line and the H2 zero-phonon line is expected if the 1.424 eV line is a local mode sideband. Since the electronic states of the C_{2v} H2 centre are non-degenerate, a local mode sideband must involve a vibrational mode whose displacements transform as the A_1 irreducible representation. The vibronic excited state then transforms as the electronic excited state, producing the same polarized stress spectra as for the zero-phonon line. Given the small anharmonicity typical of vibrations in diamond, the same uniaxial stress perturbations

Table 1. Stress parameters for the H2 band.

Transition	Stress parameters (meV GPa^{-1}) A_1	A_2	A_3
1.257 eV H2 ZPL 1.424 eV H2 LVM	−8.8	6.0	6.3
2.463 eV H3 ZPL	−8.7	6.7	6.9

are expected for a local mode sideband and for the zero-phonon line as observed, e.g. at the '5RL' band in diamond (Collins and Spear 1986).

The A_1,A_2 and A_3 parameters of the H2 system (table 1) are very similar to those of the H3 zero-phonon line (Davies *et al* 1976). The similarities are discussed in section 7. The main difference in the stress response of the two centres is that the H3 excited state interacts under stress with a higher energy level; when (111) stresses exceed 2 GPa the interaction is clearly visible for the H3 line but is not seen in the H2 band.

5. Temperature dependence and shape of the H2 band

The H2 zero-phonon absorption line is sufficiently sharp relative to the underlying absorption (figure 4(a)) that an accurate baseline is given by a cubic curve fitted to the measured absorption outside the peak. With increasing temperature the line loses integrated intensity and moves to lower energy (figure 5).

To determine the behaviour of the 1.424 eV absorption line we must allow for the step in the underlying absorption (shown clearly in the '^{12}C' spectrum of figure 4(b)). The step is caused by the cut-off of the optic-mode contribution to the H2 vibronic band. The marker labelled ν_m on figure 4(b) is drawn at the Raman energy (165.5 meV at low temperature (Nayar 1941)) above the H2 zero-phonon line for the '^{12}C' spectrum. To generate a baseline we first represent the absorption $A(\nu)$ at the cut-off of these weak optic modes as a square root form

$$A(\nu) = 0, \ \nu > \nu_m \qquad \text{and} \qquad A(\nu) \propto \sqrt{\nu_m - \nu}, \ \nu < \nu_m. \tag{2}$$

This baseline is then broadened by convolution with the zero-phonon lineshape to represent the effects of strain and thermal broadening. The zero-phonon lineshape is very close to the shape $Z(\nu) \propto 1/(a^2 + (\nu - \nu_p)^2)^2$ where ν_p is the frequency at the peak of the line and its full-width at half-height is $\Gamma = 1.287a$. With this baseline, the area of the 1.424 eV line is found to diminish with temperature in proportion to the zero-phonon line (figure 5(a)). In the limit of low temperature the ratio of the transition probabilities of the 1.424 eV line and the zero-phonon line is

$$S_{lm} = \int_{1.424} \mathrm{d}\nu \ \frac{\mu(\nu)}{\nu} \Big/ \int_{\mathrm{zpl}} \mathrm{d}\nu \ \frac{\mu(\nu)}{\nu} = 0.135 \pm 0.004 \tag{3}$$

where $\mu(\nu)$ is the absorption coefficient at photon frequency ν.

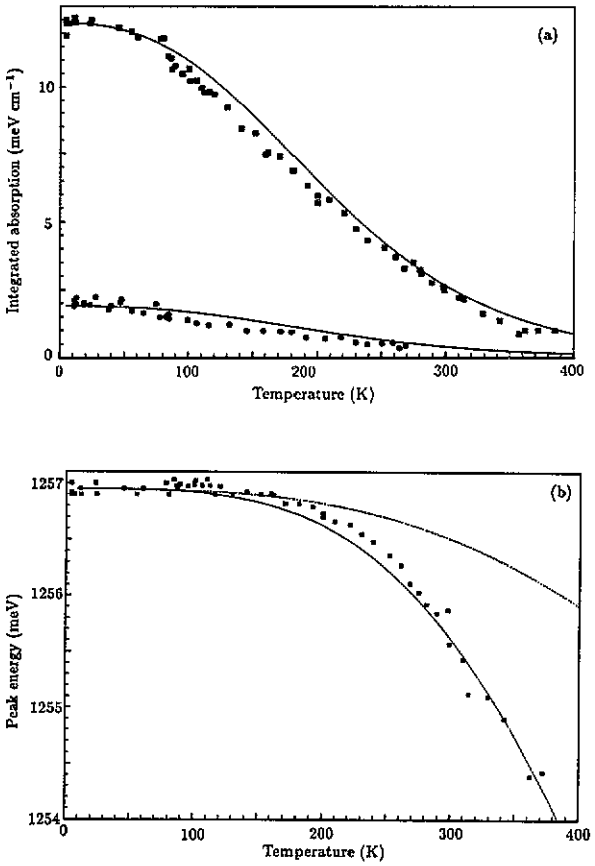

Figure 4. (a) Points show the measured absorption integrated across the zero-phonon line (stronger line) and the 1.424 eV line as functions of temperature. The lines through the data are calculated with no adjustable parameters, as described in section 5. (b) The measured energy of the peak of the H2 zero-phonon line is shown by the points. The broken line shows the contribution calculated explicitly for the effect of lattice expansion. The solid line shows the sum of the lattice expansion term and the Debye parameterization (equation (14)).

We have not obtained any data for the H2 zero-phonon line in photoluminescence. In our ^{12}C samples the absorption in the H2 zero-phonon line was sufficiently strong that the zero-phonon luminescence was partially re-absorbed, distorting the spectra (figure 1(b)).

The shape of the vibronic absorption band cannot be defined accurately given the uncertainties in the underlying absorption (figure 1(a)). An estimated bandshape is shown in figure 6(a) and is expressed as a transition probability spectrum, i.e. the measured absorption spectrum has been divided by the photon energy. The ratio S' of the transition probabilities integrated over respectively the estimated total band and the zero-phonon line is, at 2 K,

$$S' = \ln\left(\int_{\text{band}} d\nu \, \frac{\mu(\nu)}{\nu} \Big/ \int_{\text{zpl}} d\nu \, \frac{\mu(\nu)}{\nu}\right) = 3.5 \pm 0.1. \tag{4}$$

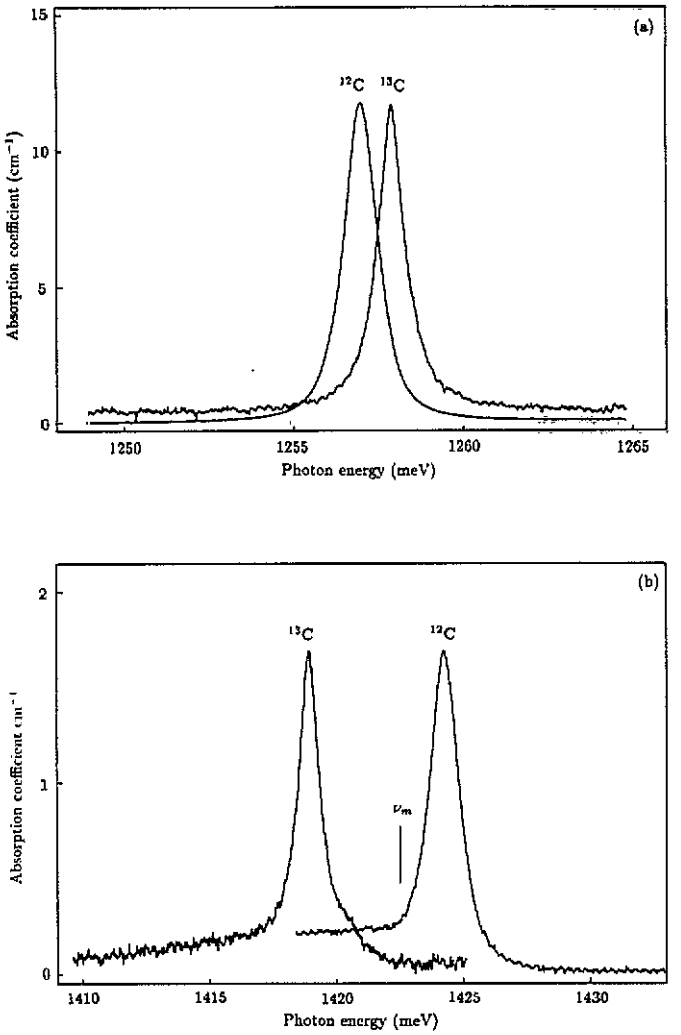

Figure 5. Comparisons of (a) the 1.257 eV line and (b) the 1.424 eV line in ^{12}C diamond with their counterparts in ^{13}C diamond. The spectra were recorded at 77 K. Absorption coefficients are shown for the ^{12}C diamond. The absorption was almost four times weaker in the ^{13}C diamond, but the lines have been scaled to approximately the same amplitude for comparison purposes. In (b) the ^{13}C spectrum is an average of 10 scans. ν_m labels the cut-off of the phonon continuum of ^{12}C diamond measured from the H2 zero-phonon line.

Since the H2 transition occurs between non-degenerate orbital states, the vibronic sideband can only involve those vibrational modes which transform as A_1 in the C_{2v} point group. The bandshape in the limit of low temperature can be written as the sum of individual phonon sidebands, the n^{th} sideband involving the creation of n randomly chosen phonons (section 13 of Maradudin 1966). Thus the n^{th} sideband $P_n(\omega)$ at the frequency ω from the zero-phonon line is the convolution of the $(n-1)^{th}$ sideband and the one-phonon sideband:

$$P_n(\omega) = \int_0^{\omega_m} \mathrm{d}x \; P_1(x) P_{n-1}(\omega - x) \tag{5}$$

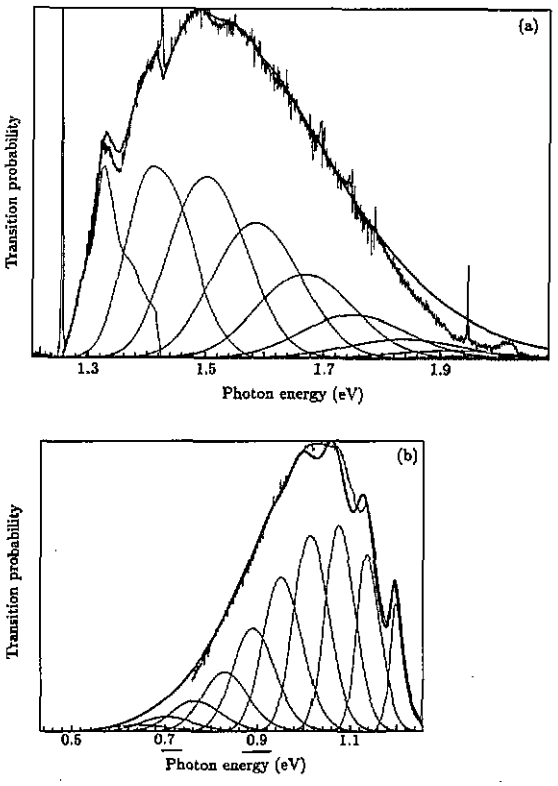

Figure 6. H2 absorption and emission bandshapes at 77 K. (a) The experimental curve (with noise) shows the estimated transition probability in the H2 absorption band of figure 1(a), after subtracting an estimated baseline. The smooth curve closely fitting it is the sum of the individual phonon components shown by the thin lines, as described in section 5. The feature at 1.945 eV is a zero-phonon line at the independent N–V complex. (b) The experimental curve (with noise) shows the transition probability in the H2 photoluminescence band, recorded at 77 K. The smooth curve closely fitting the experimental curve is the sum of the individual phonon components shown by the thin lines, as described in section 5.

where ω_m is the maximum frequency of the one-phonon processes. The relative weighting of the n^{th} phonon sideband in the total bandshape is

$$I_n = \exp(-S)S^n/n! \qquad \text{where } I_n = \int_0^{n\omega_m} d\omega\ P_n(\omega) \tag{6}$$

and where the Huang–Rhys factor S is given by the intensity in the zero-phonon line I_0 relative to the total band intensity by

$$S = \ln\left(\sum_0^\infty I_n \Big/ I_0\right). \tag{7}$$

It is convenient to treat the local mode sideband as the precursor of a new vibronic band, with a bandshape that is identical to the bandshape initiated by the H2 zero-phonon line. The total H2 absorption band has a transition probability $\exp 3.5 = 33$ times that of the zero-phonon line (equation (4)), of which a fraction 0.135 originates

in the local mode and its phonon sidebands (equation (3)). The Huang–Rhys factor for the band originating in the H2 zero-phonon line is therefore $S = 3.35$. With this value of S, and by iterative choice of a one-phonon sideband $P_1(\omega)$, equations (5)–(7) result in the fit to the bandshape shown in figure 6(a). The one-phonon contribution $P_1(\omega)$ is a broad peak with its maximum near 65 meV. $P_1(\omega)$ includes optic modes, as required for the discontinuity in the baseline under the local mode sideband.

In luminescence the one-phonon sideband peaks at only about 62 meV from the zero-phonon line, as opposed to at about 66 meV in absorption. There is also no evidence in luminescence for the local mode sideband (figure 1(b)). If the local mode is reduced in quantum energy by 6%, as for the perturbed lattice modes, its quantum of 157 meV would lie within the continuum of phonon energies of diamond (0 to 165 meV). The 'local mode' would then be expected to be broadened. Since, in the absorption spectra, the local mode contributes only 4% of the one-phonon transition probability, it could easily become an undetectable part of the luminescence band. (This situation occurs, e.g., in the '5RL' band where the local mode may be seen in luminescence but not in the absorption spectrum, Collins and Spear 1986). To simulate the luminescence band we have used the same bandshape theory as above. The measured luminescence band has been converted to a transition probability spectrum by dividing by the cube of the photon energy. Strong self-absorption of the zero-phonon line prohibits a measurement of the Huang–Rhys factor in luminescence. The best fit to the luminescence bandshape is obtained with a Huang–Rhys factor of $S_l = 4.4$ and a one-phonon bandshape $P_1^l(\omega)$ which is essentially a broad peak centred on 62 meV (figure 6(b)).

The temperature dependence of the zero-phonon intensity arises from thermal population of the vibrations of the optical centre. For the absorption data of figure 5(a), thermal equilibrium is established among the phonons in the ground electronic state, which are observed in the *luminescence* bandshape. We use the explicit relationship between $P_1^l(\omega)$ and the intensity variation (equations (13.42) and (13.45) of Maradudin 1966) :

$$I_0(T) \propto \exp\left(-b\int_0^{\omega_m} \mathrm{d}\omega\ P_1^l(\omega)(2n(\omega)+1)\right). \tag{8}$$

where $n(\omega)$ is the Bose–Einstein factor. The constant b is dependent on the normalization of P_1^l and is chosen so that I_0 contains $\exp(-S_l)$ of the intensity at 0 K. The line on figure 5(a) is calculated using equation (8) with no adjustable parameters, and gives a satisfactory fit to the variation of the H2 zero-phonon intensity. Equation (8) also fits the variation of the 1.424 eV line when scaled to the smaller absorption value at $T = 0$ K (figure 5(a)).

The temperature dependence of the energy of the zero-phonon line is shown by the points on figure 5(b). To interpret the data we first strip out the contribution from lattice expansion. From equation (1), lattice expansion produces a line-shift of

$$\Delta E_e = -(A_1 + 2A_2)(c_{11} + 2c_{12})\int_0^T \mathrm{d}T\ \alpha(T) \tag{9}$$

where α is the coefficient of linear expansion of diamond (Slack and Bartram 1975), and the elastic constants $(c_{11}+2c_{12}) = 1327$ GPa (McSkimmin *et al* 1972). The effect

of the lattice expansion can thus be calculated explicitly and is given by the broken line in figure 5(b). The remainder of the temperature dependence arises because each vibrational mode in the electronic excited state has a different frequency ω_e from its frequency ω_g in the electronic ground state. Consequently the mean energy $h\nu(T)$ of the zero-phonon line at temperature T is

$$h\nu(T) = h\nu(0) + \sum n(\omega_g)\hbar(\omega_e - \omega_g). \tag{10}$$

Here the sum is over *all* the phonon modes of the optical centre. In contrast the bandshapes and the T dependence of the zero-phonon line are determined only by those vibrations transforming as A_1 in the C_{2v} point group. The A_1 modes observed in the phonon sideband of the absorption spectrum have higher energies than those observed in the luminescence spectrum (section 3), so that for these modes $\omega_e > \omega_g$. Their effect in equation (10) is to *increase* the zero-phonon energy as T increases. The observed *decrease* in zero-phonon energy implies that other modes of the centre have lower energies in the excited electronic state than in the ground electronic state. It is not possible for us to confirm this by independent measurement.

Since we have no data on the changes of phonon energy in the unobserved modes, we will parameterize the temperature dependent shift by using a Debye spectrum of phonons. Maradudin (1966) has argued (his equation (13.30)) that, at least in the long-wavelength limit, the frequency changes would vary linearly with the frequency of the mode. We find that the phonon induced shift can be fitted using the Debye approximation

$$\Delta E_d \propto \int_0^{\omega_d} d\omega\ \omega^3 n(\omega) \tag{11}$$

where ω_d is the Debye cut-off. The solid curve in figure 5(b) shows the total shift calculated with $\hbar\omega_d = 165$ meV in equation (11) plus the expansion term ΔE_e of equation (9).

6. ^{13}C isotope effects

Figure 5 compares the zero-phonon line and the 1.424 eV line of a ^{12}C diamond with the corresponding peaks in a diamond grown from 99% ^{13}C. The zero-phonon line is shifted by

$$h\nu_{13}^0 - h\nu_{12}^0 = 0.93 \pm 0.07 \text{ meV} \tag{12}$$

to higher energy in the ^{13}C diamond, while the 1.424 eV line moves in the opposite direction:

$$h\nu_{13}^l = 1418.8 \pm 0.1 \text{ meV} \qquad \text{and} \qquad h\nu_{12}^l = 1424.08 \pm 0.05 \text{ meV}. \tag{13}$$

The differences in energies of the '1.424 eV' line and the zero-phonon line are 160.87 ± 0.07 meV for ^{13}C and 167.08 ± 0.07 meV for ^{12}C. These differences are in the ratio 0.963 ± 0.001, very similar to the ratio ($\sqrt{12/13} = 0.961$) expected for a vibration involving only carbon atoms. Taken with the uniaxial stress data (section 4)

these data strongly imply that the 1.424 eV line is a sideband of the H2 zero-phonon line produced by a local vibrational mode which involves only carbon atoms.

Part of the zero-phonon shift is caused by the change in atomic spacing between ^{12}C and ^{13}C diamond. The fractional change has been measured, with about a 10% precision, as $\Delta a/a_0 = -1.5 \times 10^{-4}$ (Holloway *et al* 1991). Combined with the data of table 1, this effect produces a shift of

$$\Delta h\nu_1 = -(A_1 + 2A_2)(c_{11} + 2c_{12})\Delta a/a_0 = +0.64 \pm 0.04 \text{ meV} \tag{14}$$

where the shift is to higher energy in ^{13}C diamond. An additional contribution to the shift arises because, in the limit of low temperature, a zero-phonon transition occurs between the zero-point vibrational levels of all modes of vibration at the centre. From equation (10) the contribution to the zero-phonon energy from the zero-point energy is $\sum(\hbar\omega_e - \hbar\omega_g)/2$. Assuming that all the frequencies change by $\sqrt{12/13}$ on going from ^{12}C to ^{13}C, the change in zero-point energy is, from equation (11),

$$\Delta h\nu_2 \propto \frac{1}{2}\left(\sqrt{12/13} - 1\right)\int_0^{\omega_d} d\omega\ \omega^3. \tag{15}$$

The constant of proportionality is obtained from the fit of equation (11) to the temperature dependence of the zero-phonon energy; with $\hbar\omega_d = 165$ meV we find $\Delta h\nu_2 = +1.14$ meV, the positive sign indicating that the shift is again to higher energy in ^{13}C diamond than in ^{12}C.

In the temperature dependence measurements, which are limited in our samples to $T < 400$ K by the loss of intensity of the zero-phonon line, there is negligible population of the higher energy modes, including the local mode phonon. If the vibrational quanta of the local mode are $\hbar\omega_e = 167$ meV and, as for the acoustic modes, 6% less for $\hbar\omega_g$, the change in zero-point energy in that one mode would produce a shift in the zero-phonon line of $\Delta h\nu_3 = -0.2$ meV. We have no information on the properties (or even existence) of other local modes.

The predicted isotope shift is the sum $\Delta h\nu_1 + \Delta h\nu_2 + \Delta h\nu_3 = +1.6$ meV, compared to the measured shift of $+0.93 \pm 0.07$ meV. It is disappointing that we cannot make more accurate estimates, but our final result has the order of magnitude and sign of the observed shift (equation (12)). The limiting factor in our analysis is the major uncertainty in the vibrational quanta $\hbar\omega_e$ and $\hbar\omega_g$ of all the vibrational modes of the H2 centre in the ground and excited electronic states.

7. Discussion and summary

We have shown (section 4) that the H2 optical transition occurs at an optical centre with the C_{2v} point group, the same as for the H3 centre, supporting the model by Mita *et al* (1990) that these two optical centres differ only in their charge states. The effects of uniaxial compressions have been shown to be quantitatively almost identical for the H2 and H3 transitions (table 1). This remarkable similarity can be justified using Lowther's model of vacancy-related centres in diamond. Lowther (1984) regarded the centres as having electonic states derived from the vacancy, in a charge state and a symmetry determined by the nitrogen atoms adjacent to it. The four sp^3 dangling bonds of a vacancy give a_1 and t_2 one-electron states in the T_d point

group. In the H3 N–V–N centre, the two N atoms contribute two electrons and lower the symmetry to C_{2v}, splitting the t_2 states into b_2, a_1 and b_1 (figure (7)). A one-electron transition is electric-dipole allowed from the A_1 irreducible representation of the $a_1^2b_2^2a_1^2$ configuration to the B_1 representation ($a_1^2b_2^2a_1^1b_1^1$), consistent with the uniaxial stress data (Davies *et al* 1976). Addition of another electron for the negative charge state of the centre produces a ground state of irreducible representation B_1 ($a_1^2b_2^2a_1^2b_1^1$) and an allowed transition to the A_1 state of $a_1^2b_2^2a_1^1b_1^2$ (figure 7). For both the H3 and H2 transitions the effects of stress are determined by the difference in response of the b_1 and a_1 one-electron states and so, in Lowther's (1984) model, are identical as observed in section 4.

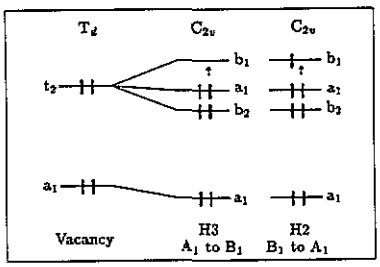

Figure 7. Effect on the one electron states of V^0 of lowering the symmetry and adding two electrons to produce the H3 $(N–V–N)^0$ centre (Lowther 1984) and adding one further electron for the H2 $(N–V–N)^-$ centre. Thick vertical lines indicate the electron occupancy of the levels in the ground state of each centre and the vertical arrows correspond to the optical transitions.

The optical data are consistent with the H2 transition occuring at the $(N–V–N)^-$ centre and the H3 transition at $(N–V–N)^0$. However, we note that in samples with strong H2 absorption, no paramagnetic resonance which could arise at the H2 centres has yet been detected (M Newton 1991 private communication).

We have shown that the H2 absorption bandshape and the temperature dependence of the zero-phonon intensity are understandable in terms of standard theory of vibronic coupling (section 5). However, there are interesting differences in the frequencies ω_e, and ω_g of the vibrational modes of the centre in the electronic excited and ground states. For the A_1 modes observed in the vibronic bandshapes $\omega_e > \omega_g$, but the temperature dependence of the zero-phonon energy establishes that for other modes $\omega_e < \omega_g$. To fit the temperature dependence of the energy of the zero-phonon line we have therefore simply used a Debye approximation (section 5). As a result our estimates of the carbon-induced isotope changes are very rough, but have the order of magnitude and sign observed (section 6).

A local vibrational mode has been identified in the absorption spectrum on the grounds of its isotope shift (section 6), its having the same response to uniaxial stresses as the zero-phonon line (section 4), and its having the same temperature dependence as the zero-phonon line (section 5). From the isotope effects the mode predominantly involves motion of carbon atoms.

The recently developed techniques for generating strong H2 absorption (Satoh 1988) now allow this 'old' band to be investigated. The study reported here is the first into the structural properties of the centre. However, further experimental work is required. In particular, studies are required on the effect on the zero-phonon line of magnetic perturbations to indicate the spin state of the centre, and nitrogen-induced

isotope changes need to be investigated to see if confirmation can be obtained of the presence of two nitrogen atoms in the centre.

Acknowledgments

We thank Dr S Satoh of Sumitomo Electric Industries for supplying the crystallographically oriented synthetic diamonds containing H2 centres, Dr H Kanda of NIRIM for growing the ^{13}C diamond used in this study, and the Science and Engineering Research Council for a maintenance grant for SCL.

References

Clark CD, Ditchburn RW and Dyer HB 1956 *Proc. R. Soc.* **237** 75
Collins A T 1980 *J. Phys. C: Solid State Phys.* **13** 2641
Collins AT and Spear PM 1986 *J. Phys. C: Solid State Phys.* **19** 6845
Davies G and Hamer MF 1976 *Proc. R. Soc.* A **348** 285
Davies G, Nazaré MH and Hamer MF 1976 *Proc. R. Soc.* A **351** 245
Davies G 1977 *Nature* **269** 498
Farrer RG 1969 *Solid State Commun.* **7** 685
Holloway H, Hass KC, Tamor MA, Anthony TR and Banholzer WF 1991 *Phys. Rev.* B **44** 7123
Kaplyanskii AA 1964 *Opt. Spectrosc.* **16** 557
Lawson SC, Collins AT, Satoh S and Kanda H 1990 *Proc. Second Int. Conf. on New Diamond Science and Technology* ed R Messier, JT Glass, JE Butler and R Roy (Pittsburgh: Materials Research Society) p 709
Lowther JE 1984 *J. Phys. Chem. Solids* **45** 127
Maradudin AA 1966 *Solid State Physics* vol 18 (New York: Academic) p 273
McSkimmin HJ, Andreatch P and Glynn P 1972 *J. Appl. Phys.* **43** 985
Mita Y, Nisida Y, Suito K, Onodera A and Yazu S 1990 *J. Phys.: Condens. Matter* **2** 8567
Nayar PGN 1941 *Proc. Ind. Acad. Sci.* **13** 284
Satoh S 1988 *European Patent No.* 88121859.8
Shcherbakova M Ya and Sobolev EV 1972 *Dokl. Akad. Nauk. SSR* **204** 851
Slack GA and Bartram SF 1975 *J. Appl. Phys.* **46** 89